Journal of Visualization, Vol. 7, No. 3 (2004) 241-248

A Realistic Coronary Artery Phantom for Particle Image Velocimetry

Featuring Injection-Molded Inclusions and Multiple Layers

Brunette, J.*[1], Mongrain, R.*[2] and Tardif, J. C.*[1]

*1 Montreal Heart Institute, Montréal, Québec, Canada.
*2 McGill University, Montreal, Quebec, Canada.

Received 28 January 2004
Revised 25 March 2004

Abstract : Myocardial infarction results from the rupture of an atherosclerotic plaque, which occurs in response to both mechanical stress and inflammatory processes. In order experimentally observe flow into atherosclerotic coronary artery morphologies, a novel technique for molding realistic compliant phantom featuring injection-molded inclusions and multiple layers has been developed. This transparent phantom allows for particle image velocimetry (PIV) flow analysis and can supply experimental data to validate computational fluid dynamics algorithms and hypothesis.

Keywords : Coronary Artery, Phantom, Plaque Rupture, Biomechanics, Computational Fluid Dynamics, PIV.

1. Introduction

Myocardial infarction (MI), causing heart attack, is an important cause of mortality and morbidity in the developed countries. Thrombosis (blood coagulation) triggered by the rupture of an atherosclerotic plaque (pathological vessel thickening creating blood flow obstruction) is the most common cause of acute coronary syndromes (myocardial infarction or unstable angina) (Lee et al., 1991). Understanding the biomechanics of the plaque, along with its physiology, is a key element to understand MI triggering. Computational studies of blood flow dynamics and its interaction with the vascular wall (fluid-structure interaction: FSI) could provide important information about velocity, pressure, stresses and strains in atherosclerotic coronary arteries. Computational models and their assumptions must be validated in order to experimentally verify their accuracy. Particle image velocimetry (PIV) is an efficient method of flow visualization to validate computational models. Existing artery phantoms do not reproduce the architecture of the normal artery layers and their pathological anisotropic inclusions. This pathology strongly affects the global mechanical behavior of the artery and the dynamics of blood flow. Arteries are composed of three layers, including the intima, the media and the adventitia. The intima is the inner most layer and is very thin. It includes a 5-10 μm thick monocellular protection film called endothelium, which actively prevents the blood from being in direct contact with the artery wall and its possible thrombogenic content. It is also involved into vasomotor activities. The intima layer however becomes thicker along with the extent of atherosclerosis and may develop inclusions that are finite volumes of (typically) lipid (at early stage) or calcium (mature plaques) or any combination. The media is a muscular layer. The adventitia is made of connective tissue and microscopic blood vessels called vasavasorum (Netter, 1987). Realistic hydraulic models (phantoms) of coronary arteries used for PIV are rare. They require being

transparent and compliant. Numerical models with simple pathological configuration have been investigated before but they included neither inclusions, nor the three layers of the artery wall. Ohayon et al. (2001) have developed a 2-dimensional numerical model with multiple layers and inclusions, but when it comes to experimental phantoms of this kind, there is very little know-how. Blown-glass tube of uniform thickness has been used for PIV experiment by Grigioni et al. (2000). Although this model had a realistic shape (it was obtained from magnetic resonance images), it was rigid and monolayer. Also, they used a water-glycerol fluid, which cannot match the refractive index of glass. To the best of our knowledge, the only coronary artery phantom featuring a flow disturbance due to pathological flow obstruction (stenosis due to atherosclerosis) with embedded inclusions (pools of pathological tissue like lipid or calcium within the artery wall) has been developed by Kobayashi et al. (2003) and Tang et al. (2001). However, this phantom was not transparent since it was developed for echographic-based analysis, therefore not suitable for PIV. Furthermore, it had only one inclusion and did not reproduce the different layers of the artery. Karino et al. (1983) developed a very elegant technique to render arteries transparent. Although they were using a tedious method of manually tracking seeded particles (one of the ancestor of more recently developed PIV technique), one can imagine that this method of transforming normal tissue into transparent material could be useful for future PIV observation. The efficiency of this technique applied to pathological tissue remains unexplored and the access to post-mortem arterial segments is neither readily available nor reproducible. Benard et al. (2003) have been using a non-realistic rectangular Plexiglas box to observe the flow in a stented coronary artery model by means of PIV. Natarajan et al. (2000) have been using a transparent cylindrical tube to reproduce an artery with embedded acrylic bumps for PIV visualization. Their model reproduced neither the different layers of the artery wall, nor its pathological flow obstruction (stenosis). They aimed to reproduce the flow in the vicinity of strut-like bumps. Finally, Bale-Glickman et al. (2003) have been using a silicone phantom molded from an ex vivo atherosclerotic carotid bifurcation geometry (obtained from magnetic resonance images) for their PIV observation. Their phantom was however mono-layered, of constant thickness, and therefore did not reproduce the wall architecture.

The molding of our phantom was performed with a set of five molds, where each mold included two halves. All molds were sharing the same male piece, also made of two halves. Each mold reproduced a different layer or inclusion. The aim of this paper is to introduce a novel technique of molding realistic transparent and compliant phantom, featuring injection molded inclusions and all arterial layers for the validation of numerical models and hypotheses or just for experimental flow analysis.

2. Materials And Methods

It is clear that each plaque has its own original configuration and that there is no universal architecture of atherosclerotic coronary artery. However, based on analysis of a large number of intravascular ultrasound sequences and insights from pathologists' experience, a typical plaque configuration has been modeled. A 50% stenosis (flow reduction as compared to sane reference segment), which represents a mild to moderate stenosis, has been chosen since plaques causing infarcts are not the most occlusive. Indeed, plaques demonstrating less than 70% occlusion are the most vulnerable and infarct related plaques are usually less than 50% occlusive on the angiography (Kullo et al., 1998). The lumen narrowing was however asymmetric, since about 75% of significant plaques are eccentric (Brown et al., 1984). This 50% lumen narrowing was modeled by a bi-Gaussian shape, on the longitudinal and transversal planes. The choice of a bi-Gaussian geometry was a simplification of the possible complexity of lesion configurations. This morphology is realistic since it can be observed in vivo. Gaussian geometry allows for controlling the width, length and amplitude of the stenosis by changing parameters into the analytic equation. It also allowed for analytic comparison obtained from computer simulations to that of experimental PIV data. The stenosis, as seen on the transversal plane of the phantom, was semicircular with soft edges that gently came down on the artery wall to avoid abrupt and unrealistic transition between the lesion and the arterial wall, which could have caused geometric singularities. Stress concentration does however

exist and can be the result of either geometrical discontinuities (due to the shape of the stenosis) (Gyongyosi et al., 1999) or physiological discontinuities (Felton et al., 1997) (due to differences of mechanical properties of the different tissues). Two distinct inclusions were incorporated into the lesion model. However, in vivo inclusions have often no clear boundaries, although certain regions have a higher percentage of one type of tissue more than one another. Lipids, calcium and fibrosis (also smooth muscle and inflammatory cells) are commonly found within plaques. A distance of 3.00 inches (76.2 mm) after upscale factor, proximal and distal to the stenosis, allowed for a sufficient access and handling of the phantom inside the observation receptacle. An additional straight segment of 16.0 inches (406 mm) proximal to the phantom an outside the receptacle insured the flow to fully develop (length>0.006*Re, (Fox and McDonald, 1999)). The reference diameter (without stenosis) was 0.75 inch (19.1 mm). A resulting scale-up factor of 6.35 was applied over anatomic dimensions in order to be able to machine and handle the phantom and also to obtain a good resolution on PIV. This factor allowed for a scaled reference diameter of 0.75 inch (19.1 mm), and inlet and outlet diameters of 1.00 inch (25.4 mm), allowing for conventional tubing and adaptor usage. Therefore, the total length of the phantom was 12.0 inches (304 mm) including 2.00 inches (51.0 mm) of lesion mimic, 3.00 inches (76.2 mm) of prestenotic segment, 3.00 inches (76.2 mm) of poststenotic segment, and 2.00 inches (50.8 mm) of adaptor segment at both ends to allow perfusion. The adventitia mimic had a thickness of 150 μm before the upscale factor, as observed in *in vivo* intravascular ultrasound (IVUS) images. There is little information in the literature about the thicknesses of the different layers of the arterial tunica whereas its histology is well documented. The media mimic had a thickness of 150 μm (unscaled). Indeed, human coronary artery media thickness is approximately 200 μm or less and the thickness of the adventitia is hard to determine because of surrounding tissues (Tardif and Lee, 1998). The media thickness however decreases along with the extent of atherosclerosis (Greenleaf, 1986). The intima mimic, which included the endothelium and the plaque, varied from 150 μm (unscaled) to 1500 μm to reproduce a 50% stenosis.

The design of the molds was created with a computer assisted design (CAD) software (ProEngineer, PTC, Needham, MA, USA) and all layers and inclusions were assembled in Pro/E. The machining of the molds was performed into aluminum blocs and was done with conventional tools (lathe, milling), whereas certain areas of complex geometry were machined on a computer numerical control (CNC). Numerical data for CNC was prepared with MasterCam, a software that specifies CNC machine mill trajectory. First, the silicone T-2 silastic translucent base was prepared by addition of 10% of T-2 curing agent catalyst (both obtained from Dow Corning Chemicals, MI, USA), which triggered the polymerization of the compound. The mixture was then degassed in a vacuum chamber. Iterative depression-compression cycles were necessary to expand air bubbles and to rupture them respectively. Once most of those bubbles were removed, the compound was spread over the two male and female pieces of the innermost layer set of mold. All parts were then replaced in the vacuum chamber. The second half of the female was placed over the first half, therefore trapping the male in between. The holding and mechanical compression of the whole set of parts for the first molding was secured with a set of 12 Allen screws. While assembling the different parts of the mold together with the screws, the previously degassed compound was compressed and the excess material was evacuated by dedicated channels. The vacuum was interrupted during the curing (chemically triggered hardening) in order to avoid any negative-pressure-induced bubble expansion. The mold was then placed in an oven chamber (Fisher Scientific, USA, model Isotemp) previously set at 80°C for two hours. Once the silicone was well set, the female parts were removed and the male, along with the set compound, was ready for the next molding step. The second part of the molding was required to create the inclusions and their compounds were also degassed, as previously described, prior to their injection. The male, along with the first intima layer molded on top of it during the first part of the molding (the intima is molded in three steps in order to trap in sandwich the embedded inclusions) was placed into the two female parts of the second mold set. The two compounds were then injected into their respective inclusion channels through the aluminum mold. These channels (small holes through the aluminum mold to inject the pressurized-compound from the syringe to a specific part of the mold) allowed the filling of the respective ellipsoidal cavity and therefore the creation of the inclusions. The silicone mixture was slowly injected (to insure that the air in the mold will be properly evacuated as the mixture fills the cavities) by means of a small

diameter syringe (3ml luer-lok, Becton Dickinson, NJ) in order to increase the injection pressure (for a given force, if the diameter doubles, the pressure drops by a factor of 4). The compound was injected until the mold cavity was filled and excess material was ejected through the overfill channel. The syringe needle used was of a relatively large diameter (BD 16G1, Becton Dickinson, NJ) to facilitate the flow of the viscous compound once the pressure was built by the syringe. Again, the mold was placed in an oven chamber at 80°C for two hours. Once the inclusions were molded, another layer of silicone was added by means of a third set of molds, therefore trapping the inclusions to simulate embedded inclusions into an atherosclerotic plaque. Again, the compound was prepared and degassed, and then spread over the male and both female halves. The mold was closed and placed in the oven chamber for curing purposes. The subsequent molding of the media and adventitia mimics were performed similarly to the previous layers, with their respective compounds and set of molds. Once all layers and inclusions were completed, compressed air was blown through specific channels within the male piece, therefore releasing the phantom from the mold.

Fluid parameters were normalized and adimensionalized according to Buckingham theorem, in order to properly reproduce physiological perfusion of the phantom. For steady flow, these parameters included consideration of the Reynolds number (Re), that represents the ratio of the inertial over viscous forces ($\mathrm{Re} = \frac{\rho u D}{\mu}$), and the Euler number ($Eu = \frac{P}{\rho u^2}$), which is important if pressure is a concern. The Re number within a coronary artery must remain the same within the phantom. This can be achieved by considering the upscaled geometry and by adjusting the amplitude of the flow in conjunction with the viscosity. The refractive index of silicone was 1.43 and the fluid in which it was perfused and immersed had a similar refractive index in order to avoid optical artefacts during PIV acquisition (Nguyen et al., 2003). Refractive indices were measured on a refractometer (Fisher Scientific, model 334620). A transparent fluid having similar refractive index to that of silicone was created by means of a mixture containing 60% of glycerol and 40% of water. The viscosity of that mixture was 14.5 mPa.s at 20°C as evaluated with a viscoelastometer (Bohlin Instruments, CVO 120 high resolution, NJ, USA) and the density was 1114 Kg/m3. The Reynolds number of the model was similar to that of coronary arteries (Re=194), based upon a coronary artery reference diameter of 3 mm with a 1.53X10-6 m3/s flow. The phantom was immersed in a transparent enclosure made of polycarbonate, filled and perfused with the described glycerol mixture, and the bath pressure was adjusted by means of controlled air pressure connected to the observation receptacle. The phantom was also perfused with the same glycerol mixture than the immersion bath, but some particles of titanium (TiO2), having a nominal size of 5 μm, were included in order to reflect some laser light for displacement tracking purposes. The phantom, enclosure, bath and flow were all transparent, therefore allowing appropriate optical conditions for PIV acquisition. Receptacle walls were perpendicular to the laser beam to avoid optical artefacts like reflection or refraction due to refractive indices mismatch. Indeed, refraction is governed by the Snell-Descartes law stated as follow: $n_1 \sin(\theta_1) = n_2 \sin(\theta_2)$, where n_1 and n_2 are the refractive indices on each side of the interface between two materials penetrated by a light beam, and θ_1, θ_2 are their respective angles of approach in respect with an axis normal to the interface. Therefore, there is no refraction phenomenon if either the light beam is perpendicular to the interface or the refractive indices are the same.

3. Results

A set of five complementary molds was created from aluminum blocks. Each mold reproduced either an artery layer or inclusions. Figure 1(A): Five molds were machined from aluminum blocks, for a total of 10 halves of female molds (five sets of female molds, 1 to 5) and a two-part male (bottom piece). The male was utilized along the whole molding process whereas each female molds were used to reproduce the three layers of the arterial tunica and two inclusions. Figure 1(B): Illustration of the resulting phantom as seen from the inside. A 50% area occlusion can be observed. The two white arrows indicate locations of the two inclusions (one larger than the other) that have been slightly

stained for illustration only (normally fully transparent). The black circle indicates the soft transition between the bi-Gaussian occlusion and the mock artery wall. Figure 1(C): Picture of the phantom as seen from the top (Fig. 1(C)-top) and from aside (Fig. 1(C)-bottom). The bottom view reveals the 50% area occlusion and its Gaussian geometry. The molding of the different layers and inclusions was performed with an add-on fashion, in which the male-piece of the mold was utilized along the whole molding process. Figure 2 illustrates the phantom installed in its receptacle filled with a 60% glycerol and 40% of water. The receptacle was sealed with Allen keys in order to be able to pressurize either the perfused phantom or the immersing bath. A one inch (25.4mm) tube installed on top of the receptacle allowed gathering possible air bubbles to avoid deterioration of the flow visualization. The phantom (delimited by the white dotted lines) was immersed into a liquid made of glycerol and water. This mixture had a refractive index similar to that of the silicone used to fabricate the phantom in order to avoid optical artefacts. The 532 nm wavelength green beam (see white arrow) allows for illumination of seeded Titanium dioxide and tracking of their displacement within the region of interest. Figure 3 (top) represents a typical image acquired by means of particle image velocimetry. Illustration of the fluid dynamics into a 50% occlusive stenosis of an atherosclerotic vascular phantom. The vessel morphology is delimited by the white dotted line. The top panel of the illustration represents a longitudinal picture of the phantom illuminated by a laser sheet (500 µm thick nominal laser beam). Small white dust-like particles are actually the Titanium dioxide reflectors mixed with the circulating flow. The tracking of those laser-illuminated particles allowed estimating the velocity of the fluid, using a cross-correlation algorithm. The bottom panel of the illustration is the resulting image pair cross-correlation analysis of the flow in the center plane of the arterial phantom. The isocontours reveal the relative (adimentionalized) distribution of the axial velocity. The fluid, going from left to right, strongly accelerates as it enters into the stenosis, where it reaches a maximum. The fluid thereafter decelerates as the vessel diameter increases. A stagnation zone can be observed on the upper right half of the vessel, facilitating the physiologic development of the pathologic flow obstruction by means of shear stress decrease.

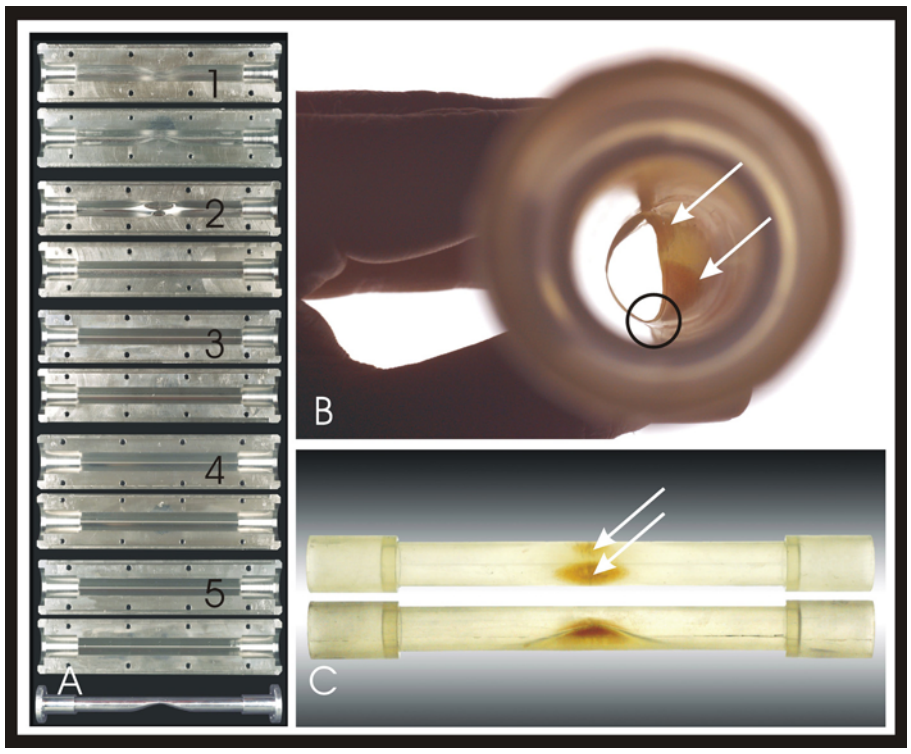

Fig. 1. Phantom fabrication.

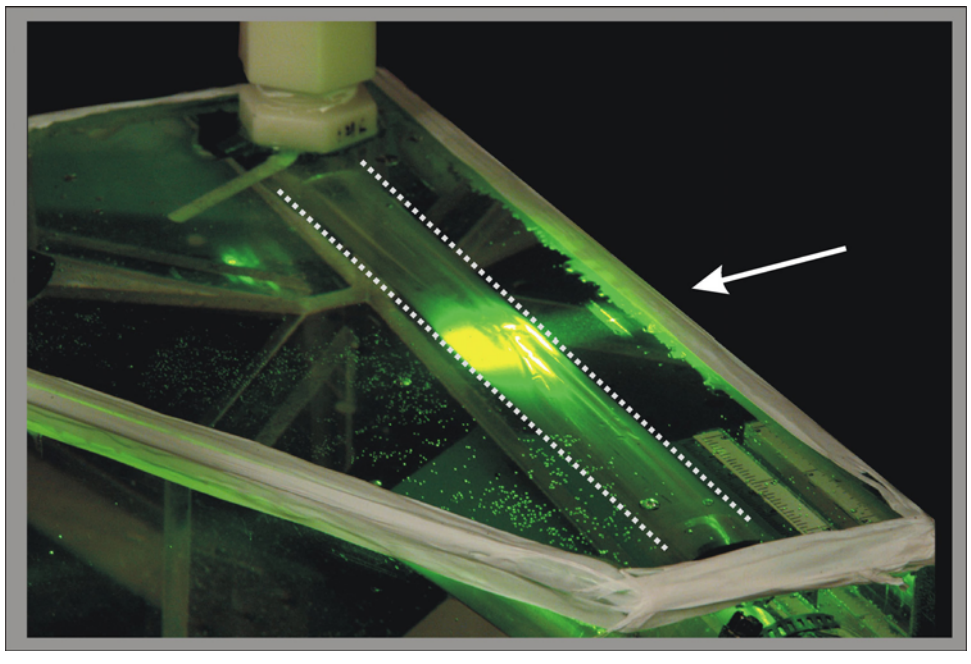

Fig. 2. Mounting and observation of the immersed phantom.

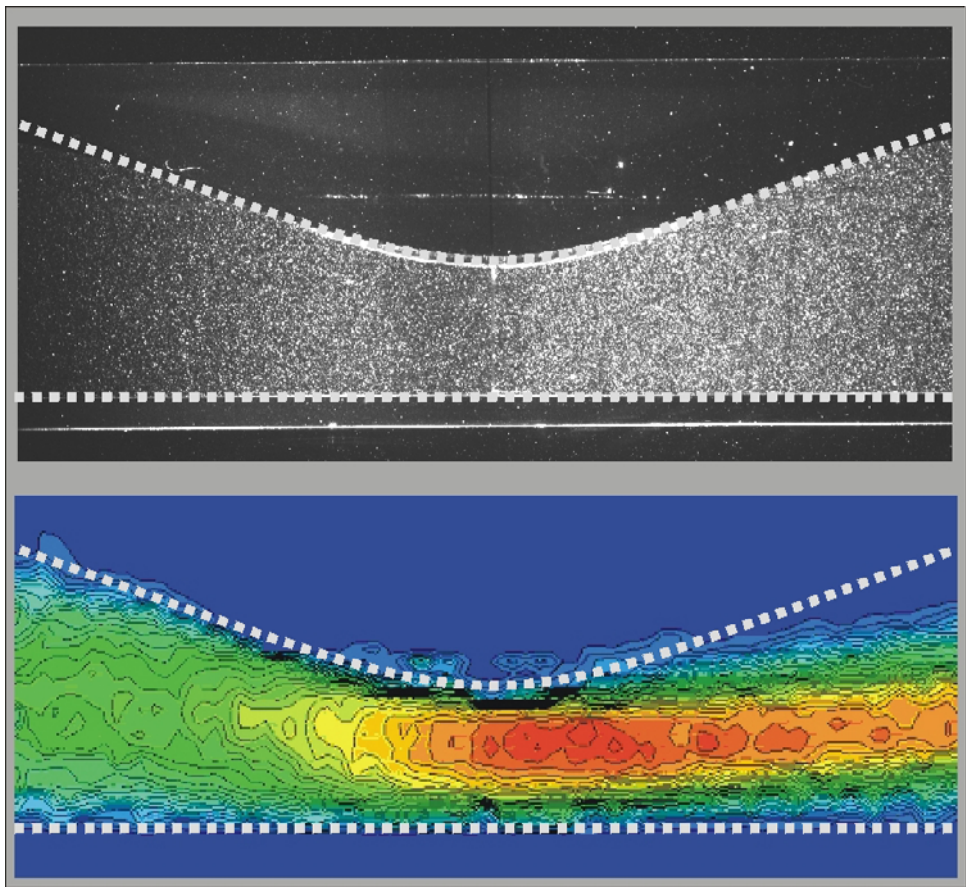

Fig. 3. Flow dynamics in a coronary artery stenosis replica.

4. Discussion

A novel method to create an anatomically correct phantom, compliant and having refractive index that can be matched, featuring injection molded inclusions and reproduction of all arterial layers from a 12-part aluminum mold was developed. Its transparency allowed for laser particle image velocimetry (PIV) and therefore experimental flow visualization for velocity field assessment. Although the method of increasing the outside pressure provided some mechanical effects of the surrounding tissue, it is clear that the imposition of a uniform, isotropic hydrostatic pressure did not perfectly reproduce the complexity of the surrounding tissues. The isotropy of the silicone did not reproduce the oriented arrangement of the artery, especially that of the media, of which muscular fibers are oriented in a tangential fashion, and the complexity of the plaque. The importance of this limitation is however attenuated by the progressive thinning of the media that occurs with atherosclerosis (Gussenhoven et al., 1991). Also, the silicone is a relatively elastic material whereas biological tissues have some viscoelastic behavior. The impact of the surrounding tissues was incorporated into the perfused model by addition of an air pressure feature that increased the pressure outside the artery wall. The pressure was adjusted so that the lumen diameter change along the cardiac cycle reached the desired value. This diameter variation decreases with age and degree of atherosclerosis (Berry et al., 2000), and may vary from 5%, as observed in the physiologic range of atherosclerotic arteries, to 10% for more compliant vessels (Shaaban and Duerinck, 2000).

Our team is presently working on a real size multilayer coronary artery phantom with inclusions, reproducing mechanical properties of in vivo arteries, aimed to test percutaneous transluminal angiography devices. Different materials and additives, like alginate, acrylamide or agar (Brunette et al., 2001), encapsulated or not, are under investigation to improve the different mechanical property possibilities within the phantom. A good reproduction of the plaque mechanical properties will allow to better reproduce the mechanics of plaque rupture (Brunette et al., 2003).

5. Conclusion

Accurate phantom (structure mimic) fabrication can be performed by means of injection molding. The technique of molding in multiple steps allows for complex anisotropic structure reproduction. Particle image velocimetry can be performed to investigate transparent phantoms reproducing *in vivo* structure morphologies, providing proper refractive index matching of the phantom, bath and perfusion. Experimental data can supply validation of numeric models and provide new insights to scientists.

Acknowledgments

The authors would like to thank Mr. N.Verzeni (McGill engineering), for his great contribution into the manufacturing and the Pro/E design of the phantom, and Mr. P.Glass for his assistance.

References

Bale-Glickman, J., Selby, K., Saloner, D. and Savas, O., Experimental flow studies in exact-replica phantoms of atherosclerotic carotid bifurcations under steady input conditions, J. Biomechanics, 125-1 (2003), 38-48.

Benard, N., Coisne, D., Donal, E. and Perrault, R., Experimental study of laminar blood flow through an artery treated by a stent implantation: characterisation of intra-stent wall shear stress, J. Biomechanics, 36 (2003), 991-998.

Berry, J. L., Santamarina, A., Moore, J. E., Roychowdhury, S. and Routh, W. D., Experimental and computational flow evaluation of coronary stents, Ann Biomed Eng., 28-4 (2000), 386-398.

Brown, B. G., Bolson, E. L. and Dodge, H. T., Dynamic mechanisms in human coronary stenosis, Circulation, 70-6 (1984), 917-922.

Brunette, J., Mongrain, R., Cloutier, G., Bertrand, M., Bertrand, O. F. and Tardif, J. C., A novel realistic three-layer phantom for intravascular ultrasound imaging, Int. J. Card Imaging, 17 (2001), 371-381.

Brunette, J., Mongrain, R., L'Allier, P. L., Bertrand, O. F., Grégoire, J. and Tardif, J. C., Intravascular imaging and the biomechanics of plaque rupture, Journal of Clinical Engineering, 28-3 (2003), 163-173.

Felton, C. V., Crook, D., Davies, M. J. and Oliver, M. F., Relation of plaque lipid composition and morphology to the stability of human aortic plaques, Arterioscler Thromb Vasc Biol, 17 (1997), 1337-1345.

Fox, R. W. and McDonald, A. T., Introduction to fluid mechanics; Fifth edition, In: John Wiley & sons, editor. 0-471-12464-8, 1999.

Greenleaf, J. F., Tissue characterization with ultrasound, (1986) CRC Press.
Grigioni, M., Amodeo, A., Daniele, C., D'Avenio, G., Formigari, R. and Di Donato, R. M., Particle image velocimetry analysis of the flow field in total cavopulmonary connection, Artificial organs, 24-12 (2000), 946-952.
Gussenhoven, E. J., Frietman, P., The S. H., van Suylen, R. J., van Egmond, F., Lancée, C. T., Van Urk, H., Roelandt, J., Stijnen, T. and Bom, N., Assessment of medial thinning in atherosclerosis by intravascular ultrasound, Am. J. Cardiol, 68 (1991), 1625-1632.
Gyongyosi, M., Yang, P., Hassan, A., Weidinger, F., Domanovits, H., Laggner, A. and Glogar, D., Coronary risk factors influence plaque morphology in patients with unstable angina, Coronary Artery Dis, 10 (1999), 211-219.
Karino, T. and Motomiya, M., Flow visualization in isolated transparent natural blood vessels, Biorheology, 20 (1983), 119-127.
Kobayashi, S., Tsunoda, D., Fukuzawa, Y., Morikawa, H., Tang, D. and Ku, D. N., Flow and compression in arterial models of stenosis with lipid core, ASME 2003 (Florida), (2003-6), 497-498.
Kullo, I. J., Edwards, W. D. and Schwartz, R. S., Vulnerable plaque: pathobiology and clinical implications, Ann. Intern Med., 129 (1998), 1050-1060.
Lee, R. T., Grodzinsky, A. J., Frank, E. H., Kamm, R. D. and Schoen, J. F., Structure-dependent dynamic mechanical behavior of fibrous caps from human atherosclerotic plaques, Circulation, 83-5 (1991), 1764-1770.
Natarajan, S. and Mokhtarzadeh-Dehghan, M. R., A numerical and experimental study of periodic flow in a model of a corrugated vessel with application to stented arteries, Med. Eng. Phys. 22 (2000), 555-566.
Netter, F. H., The CIBA collection of medical illustrations, (1987), Yonkman F.
Nguyen, T. T., Mongrain, R., Brunette, J., Biadillah, Y., Bertrand, O. F. and Tardif, J. C., A method for matching the refractive index and kinematic viscosity of a blood analog for PIV investigations in hydraulic cardiovascular models, J. Biomechanics, (2003) (accepted).
Ohayon, J., Teppaz, P., Finet, G. and Rioufol, G., In-vivo prediction of human coronary plaque rupture location using intravascular ultrasound and finite element method, Coronary Artery Dis, 12 (2001), 655-663.
Shaaban, A. M. and Duerinck, A. J., Wall shear stress and early atherosclerosis: a review, Am. J. Radiology, 174 (2000), 1657-1665.
Tang, D., Yang, C., Kobayashi, S. and Ku, D. N., Steady flow and wall compression in stenotic arteries: A three-dimensional thick-wall model with fluid-wall interactions, J. Biomed Eng., 1 A.D. 123, 548-557.
Tardif, J. C. and Lee, H. S., What's new in cardiovascular imaging? Applications of intravascular ultrasound (IVUS) in cardiology, (1998), 133-148, Kluwer academic.

Author Profile

Mr. Jean Brunette is currently completing his PhD Biomedical Engineering at the Montreal Heart Institute under the University of Montreal Faculty of Medicine program. He did his master degree in Biomedical Engineering at the École Polytechnique of Montreal on intravascular ultrasound imaging. He is presently working on experimental blood dynamics into atherosclerotic coronary arteries and development of cardiovascular devices. Mr. Brunette is currently preparing his postdoctoral industrial fellowship in stent deployment and cryoablation interventions.

Dr. Rosaire Mongrain is an Assistant Professor in Mechanical Engineering at McGill University. He is also a researcher at the Montreal Heart Institute and shares a Biomechanics Laboratory with clinical researchers and basic scientists. He completed his PhD at the École Polytechnique of Montreal in biomedical engineering on blood dynamics and a postdoctoral fellowship at Brigham's Women Hospital in interventional radiology. Dr. Mongrain research interests include blood flow dynamics, cardiovascular rheology, circulatory disorders and the design and improvement of cardiovascular devices.

Dr. Jean-Claude Tardif is an associate professor of Montreal faculty of medicine at the Montreal Heart Institute, where he also serves as a cardiologist and Director of Research. Dr. Tardif is holder of a chair on atherosclerosis created by the Pfizer pharmaceutical society, Health Research Canada and the University of Montreal. Conducting 40 people within his team, he is specialized into antioxidants and intravascular ultrasound imaging. He wrote numerous articles in prestigious journals like the New England Journal of Medicine and has been stated as one of the most promising researchers of the new generation by the American Time magazine.